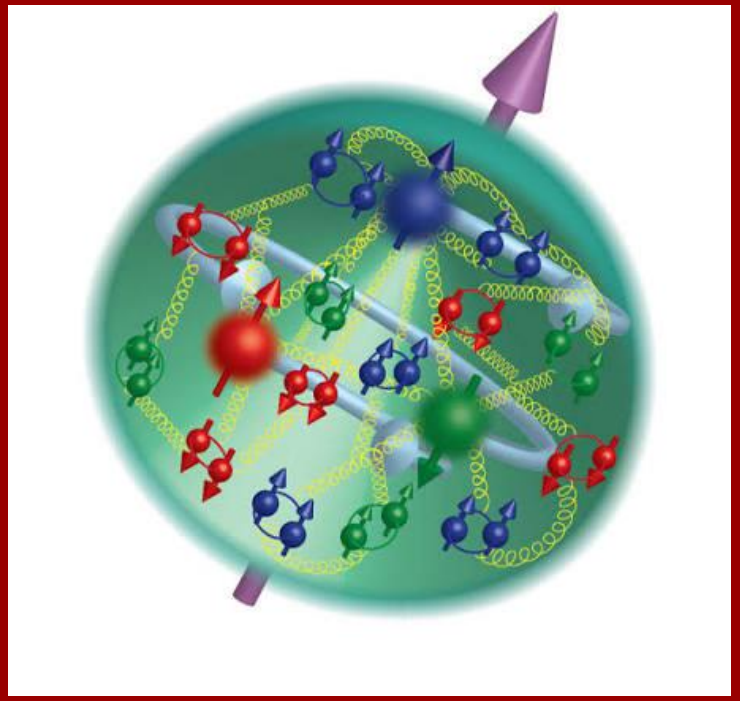

The Structure of the Nucleon

Introduction

- The structure of the nucleon is investigated through lepton $\ell = (e, \mu, \nu)$-Nucleon (N) scattering
- Neglecting lepton mass, in N rest frame
  - Four momenta:
    - $k = (E, E, 0,0)$: incoming lepton
    - $k' = (E', E'cos\theta, E'sin\theta, 0\ )$: outgoing
    - $p = (M, 0,0,0)$ target nucleon
    - p' , recoil after scattering, with $p'^2 = p'_\rho p'^\rho = W^2$
    - $q = k - k' = p' - p$ virtual photon

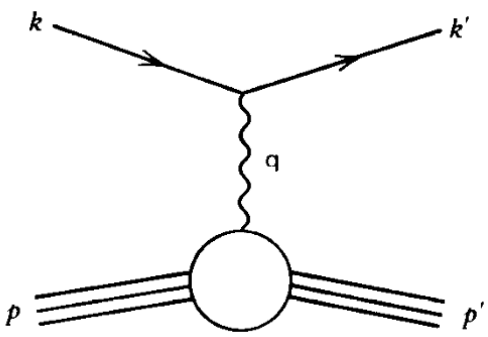

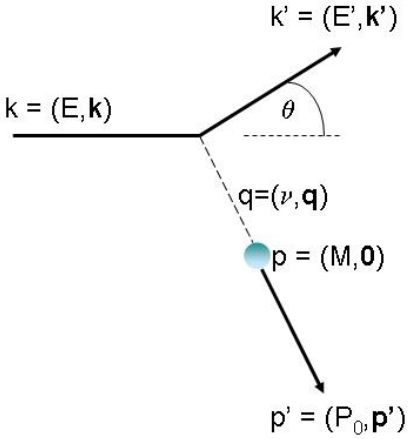

Kinematics

- $q_0 = E - E' = \nu$
- $q^2 = (k - k')^2 = -4EE' \sin^2 \theta/2$
- $W^2 - M^2 = q^2 + 2M\nu$

– Elastic:

- $W^2 = M^2 \rightarrow q^2 = -2M\nu$

– Resonances:

- $W^2 = M(\Delta), M(N'), \ldots$

– Continuum

- $W^2 > 2\ GeV$

In all regimes the scattering can be studied **measuring only the scattered electron properties.**

In elastic events, for fixed beam energy, **only one variable is needed** (e.g. θ):
$E' = E/\,(1 + E/M\,(1 - cos\theta))$

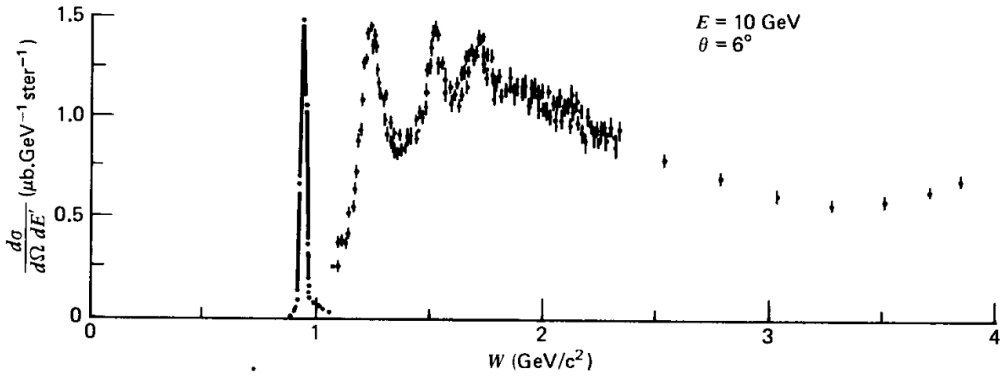

Fig. 8.6 The ep → eX cross section as a function of the missing mass W. Data are from the Stanford Linear Accelerator. The elastic peak at $W = M$ has been reduced by a factor of 8.5.

The virtual photon as a probe

- Diffraction: the photon can investigate structues not smaller than its Compton wavelength
  - $\lambda = \frac{\hbar}{|\vec{q}|} \sim \frac{\hbar c}{E} \sim 200\ MeV\ fm\ /\ E$
    - $E \sim 100\ MeV \rightarrow \lambda \sim 2\ fm$ nuclei
    - $E \sim 1\ GeV \rightarrow \lambda \sim 0.2\ fm$ nucleons
    - $E \gg 1\ GeV \rightarrow \lambda \ll 0.1\ fm$ resolve quarks

Note: in the following I often use $Q^2 = -q^2$

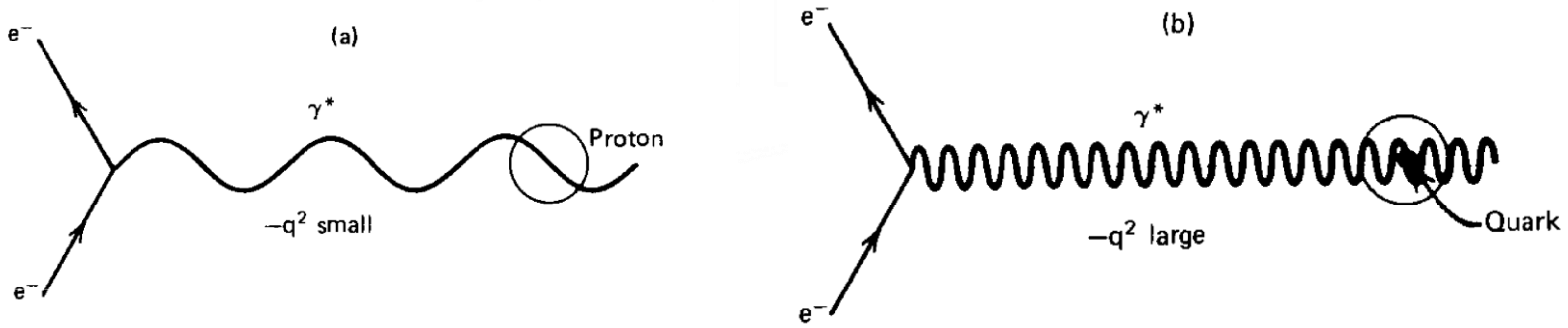

Cross sections

- $\frac{d\sigma_R}{\mathrm{d}\Omega} = \frac{(zZe^2)^2}{16E^2 \sin^4 \theta/2}$
  - Rutherford: spinless beam, spinless point-like static source
- $\frac{d\sigma_M}{d\Omega} = \left(\frac{d\sigma_R}{d\Omega}\right)\frac{E'}{E}\left(1 - \beta \sin^2 \frac{\theta}{2}\right) \simeq \left(\frac{d\sigma_R}{d\Omega}\right)\frac{E'}{E}\cos^2 \theta/2$
  - Mott : spin ½ beam, recoil spinless target
  - E′/E : target recoil
  - $\cos^2 \theta/2$ term suppresses backward scattering ($\theta = \pi$), due to:
    - ✓ Conservation of angular momentum (always true)
    - ✓ Conservation of helicity (only for ultrarelativistic particles)
- $\frac{d\sigma_{1/2}}{d\Omega} = \frac{d\sigma_M}{d\Omega}\left(1 + 2\tau \tan^2 \theta/2\right)$
  - Spin ½ target as well, $\tau = Q^2/4M^2$

A note on spin

- The lepton momentum provides the quantization axis before (z) and after (z') the scattering
- Scattering: transition of the 3rd component of J: $j_z \rightarrow j'_z$
  - $M_{fi}(\theta) \propto < J', j'_z \left| e_2^{-iJ_y\theta} \right| J, j_z > = d^J_{j_z, j'_z}(\theta)$ → Wigner matrix
- Helicity $h = \vec{\sigma} \cdot \vec{p} / p = \pm \frac{1}{2}$ is the projection of the fermion spin along its momentum
- It is conserved for an ultra-relativistic particle

Spin j=½ beam on spinless target

- Conservation of angular momentum j_z and helicity h vetoes backward scattering



$j_z = +1/2$ is conserved but helicity is reversed $(+1/2 \rightarrow -1/2)$.
Vetoed for ultrarelativistic beam particles



$h = +1/2$ is conserved but angular momentum is flipped $(+1/2 \rightarrow -1/2)$.
Always vetoed

- This introduces the $\cos^2 \theta/2$ term in $\sigma(Mott)$enhancing forward scattering

Spin j=½ beam on j=1/2 target

- $j_z = j_{z,b} + j_{z,t}$ can be either 0 or 1

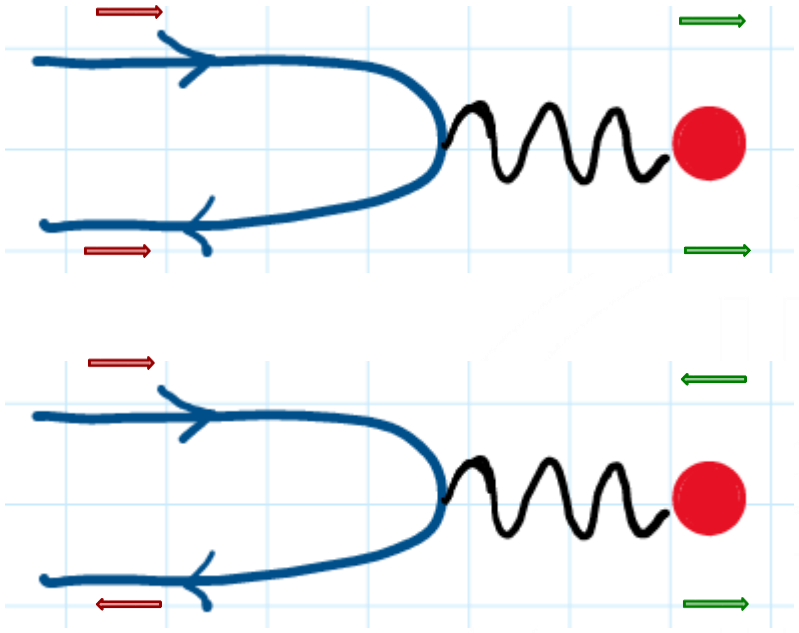

$j_z = +1$ is conserved but helicity is reversed $(+1/2 \rightarrow -1/2)$.
Same as above gives $\boldsymbol{\cos^2\theta/2}$

$j_z = 0$ allows conservation of both j_z and h.
Adds $-\frac{q^2}{2M^2}\boldsymbol{\sin^2\theta/2}$ term

- Backward scattering takes place due to spin flip of the target
- It's a magnetic interaction
- The $-q^2/2M^2$ term is due to the target magnetic moment $\vec{\mu}_t = g\frac{e}{2M}\vec{J}$, where g is the gyromagnetic factor, g=2 for a point-like spin ½ fermion in the Dirac theory

Not point-like spinless target (nuclei, π^+, K^+)

- Introduce a **form factor** ($F(|\vec{q}|^2)$, which can be interpreted as the **Fourier transform** of the charge density distribution $\rho(r)$ for $|\vec{q}|^2 \sim 0$

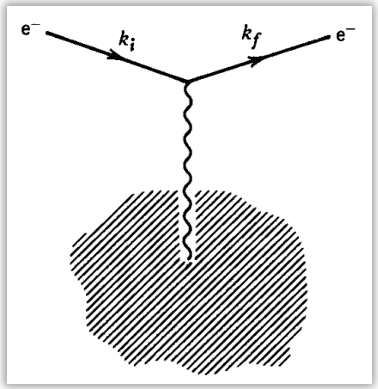

  - $\frac{d\sigma_M}{d\Omega} = \left(\frac{d\sigma_R}{d\Omega}\right)\frac{E'}{E}\cos^2\theta/2 \quad F(|\vec{q}|^2)$
  - $F\left(\overrightarrow{|q|^2}\right) = \int d^3r\, \rho(r) e^{i\vec{q}\cdot\vec{r}} = 2\pi \int d\, cos\theta \int r^2 dr\, \rho(r) e^{i\vec{q}\cdot\vec{r}}$
- … with the normalization condition
  - $\int d^3r\, \rho(r) = 4\pi \int r^2 dr\, \rho(r) = 1 \rightarrow F(0) = 1$
- For $|\vec{q}|^2 \sim 0$ we can Taylor expand F:
  - $F(|\vec{q}|^2) \simeq F(0) + \frac{dF(|\vec{q}|^2)}{d|\vec{q}|^2}|\vec{q}|^2 + \cdots = 1 - \frac{1}{6} < r^2 > |\vec{q}|^2$

Form factor and geometry

- The analytic form of F tell us about the shape of the charge distribution, through a Fourier anti-transformation
- The slope close to $|\vec{q}|^2 \sim 0$ gives $6 < r^2 >$

Table 5.1. Connection between charge distributions and form factors for some spherically symmetric charge distributions in Born approximation.

Charge distribution $f(r)$		Form Factor $F(q^2)$	
point	$\delta(r)/4\pi$	1	constant
exponential	$(a^3/8\pi)\cdot\exp(-ar)$	$\left(1+q^2/a^2\hbar^2\right)^{-2}$	dipole
Gaussian	$\left(a^2/2\pi\right)^{3/2}\cdot\exp\left(-a^2r^2/2\right)$	$\exp\left(-q^2/2a^2\hbar^2\right)$	Gaussian
homogeneous sphere	$\begin{cases} 3/4\pi R^3 & \text{for } r \le R \\ 0 & \text{for } r > R \end{cases}$	$3\alpha^{-3}(\sin\alpha - \alpha\cos\alpha)$ with $\alpha = \lvert q\rvert R/\hbar$	oscillating

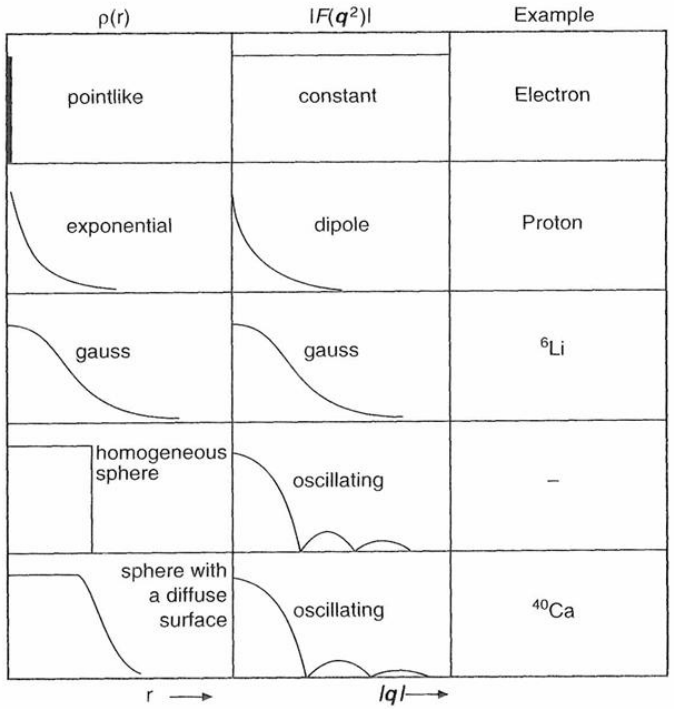

Examples

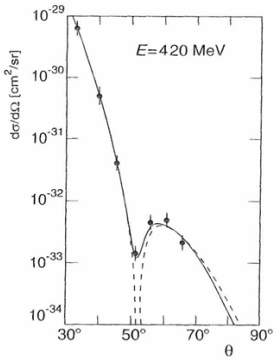

Fig. 5.5. Measurement of the form factor of ^{12}C by electron scattering (from [Ho57]). The figure shows the differential cross-section measured at a fixed beam energy of 420 MeV, at 7 different scattering angles. The dashed line corresponds to scattering of a plane wave off an homogeneous sphere with a diffuse surface (Born approximation). The solid line corresponds to an exact phase shift analysis which was fitted to the experimental data.

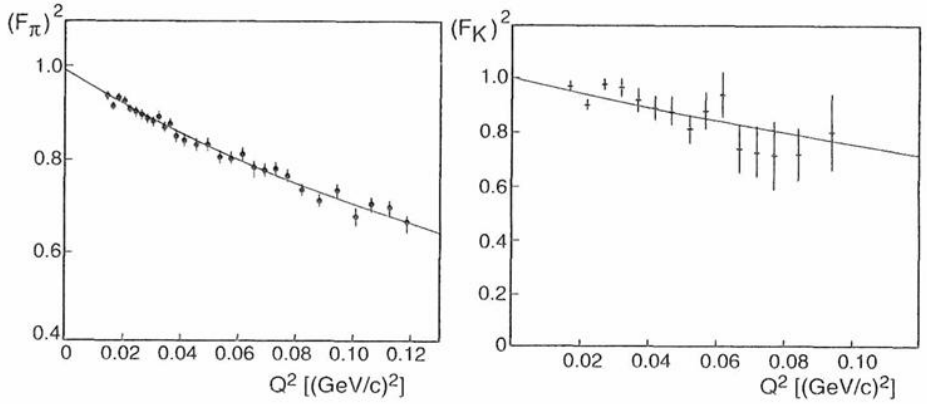

Fig. 6.4. Pion and kaon form factors as functions of Q^2 (from [Am84] and [Am86]). The solid lines correspond to a monopole form factor, $(1 + Q^2/a^2\hbar^2)^{-1}$.

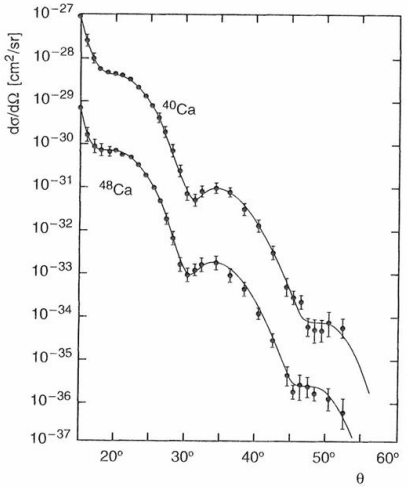

Fig. 5.7. Differential cross-sections for electron scattering off the calcium isotopes ^{40}Ca and ^{48}Ca [Be67]. For clarity, the cross-sections of ^{40}Ca and ^{48}Ca have been multiplied by factors of 10 and 10^{-1}, respectively. The solid lines are the charge distributions obtained from a fit to the data. The location of the minima shows that the radius of ^{48}Ca is larger than that of ^{40}Ca.

C and Ca oscillating form factor shape hints that their charge distribution is almost uniform within a sphere of radius $r \sim$ a few fm

Pion and kaon ff are measured scattering π / K beams off *electrons* bound in atoms. Best fits are provided by a dipole function. Its Fourier transform is an exponential (see previous slide) with

$$\sqrt{< r_\pi^2 >} = 0.67 \pm 0.02\ fm$$

$$\sqrt{< r_K^2 >} = 0.58 \pm 0.05 fm$$

The Rosenbluth Cross Section

- Two ff are needed, accounting for the distributions of the *electric charge* and *magnetic dipole moment*
  - $\frac{d\sigma_{Ros}}{d\Omega} = \left(\frac{d\sigma_M}{d\Omega}\right)\left(\, a(Q^2) + b(Q^2)\tan^2\theta/2 \,\right)$
    - $a(Q^2) = \left(G_E^2(Q^2) + \tau G_M^2(Q^2)\right)/(1+\tau)$
    - $b(Q^2) = 2\tau\, G_M^2(Q^2)$
    - $Q^2 = -q^2 = 4EE'\sin^2\theta/2$
    - $\tau = Q^2/4M^2$

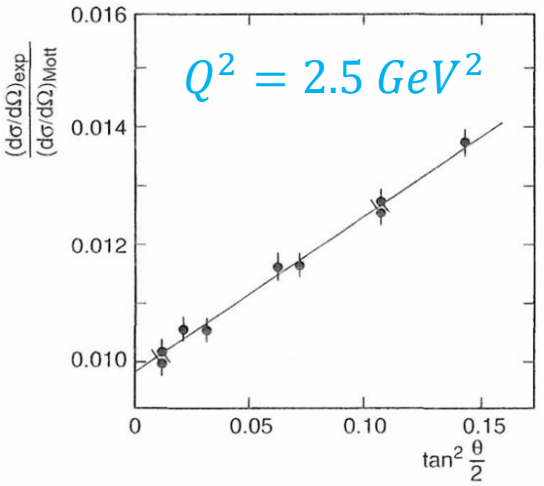

- G_E^2, G_M^2 are obtained with a linear fit to $d\sigma_{Ros}/d\sigma_M$ at fixed Q^2
  - A plot for each value of Q^2
  - Elastic scatter: must use events with different beam energies (E) to produce a single plot

Proton, Neutron structure

- All *ff* can be parameterized by the same *dipole function:*
  - $G_E^p(Q^2) = \frac{G_M^p(Q^2)}{g_p} = \frac{G_M^n(Q^2)}{g_n} = G^{dipole}(Q^2) = \left(1 + \frac{Q^2}{a^2}\right)^{-2}$
- Its Fourier anti-transform gives the spatial distribution of the charge and magnetic moment densities:
  - $\rho(r) = \rho(0)e^{-ar}$

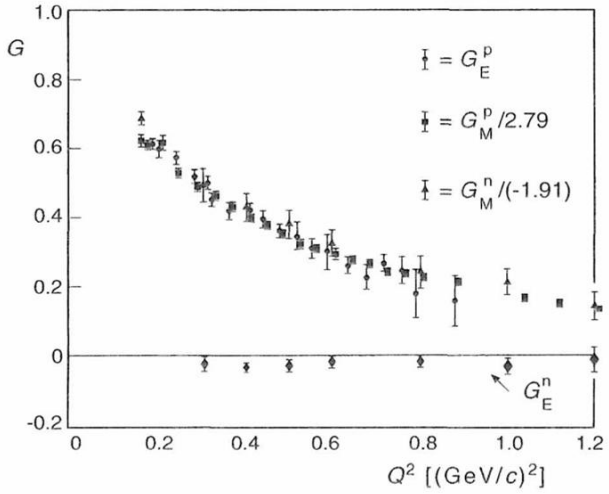

Fig. 6.2. Proton and neutron electric and magnetic form factors as functions of Q^2. The data points are scaled by the factors noted in the diagram so that they coincide and thus more clearly display the global dipole-like behaviour [Hu65].

Proton, Neutron structure

- All *ff* can be parameterized by the same *dipole function:*
  - $G_E^p(Q^2) = \frac{G_M^p(Q^2)}{g_p} = \frac{G_M^n(Q^2)}{g_n} = G^{dipole}(Q^2) = \left(1 + \frac{Q^2}{a^2}\right)^{-2}$
    - $g_p = \frac{\mu_p}{\mu_N} = +2.79$ is the *proton anomalous gyromagnetic factor*
    - $g_n = \frac{\mu_n}{\mu_N} = -1.91$ is the *neutron anomalous gyromagnetic factor*
    - $\mu_N = \frac{e}{2M_p} = 3.1525 \cdot 10^{-14} MeVT^{-1}$
- Its Fourier anti-transform gives the distribution of the charge and magnetic moment densities:
  - $\rho(r) = \rho(0)e^{-ar}$
    - $a = 4.27\ fm^{-1} = 0.824\ GeV \rightarrow \sqrt{< r_N^2 >} = \sqrt{12/a^2} = 0.81\ fm$

Deep Inelastic Scattering

- At large $Q^2 (> 2\ GeV^2)$ inelastic scattering dominates
  - $W^2 - M_p^2 = -Q^2 + 2M_p\nu \geq 0$
- The *form factors* become *structure functions,* described in terms of $Q^2 (= 4EE' \sin^2 \theta/2)$ and $\nu = (E - E')$ which are now two *independent variables* !
- We introduce also the parameter x which measures the deviation from elasticity
  - $x = \frac{Q^2}{2M_p\nu} \rightarrow 0 \leq x \leq 1$
    - ($x = 1 \rightarrow$ elastic scattering)

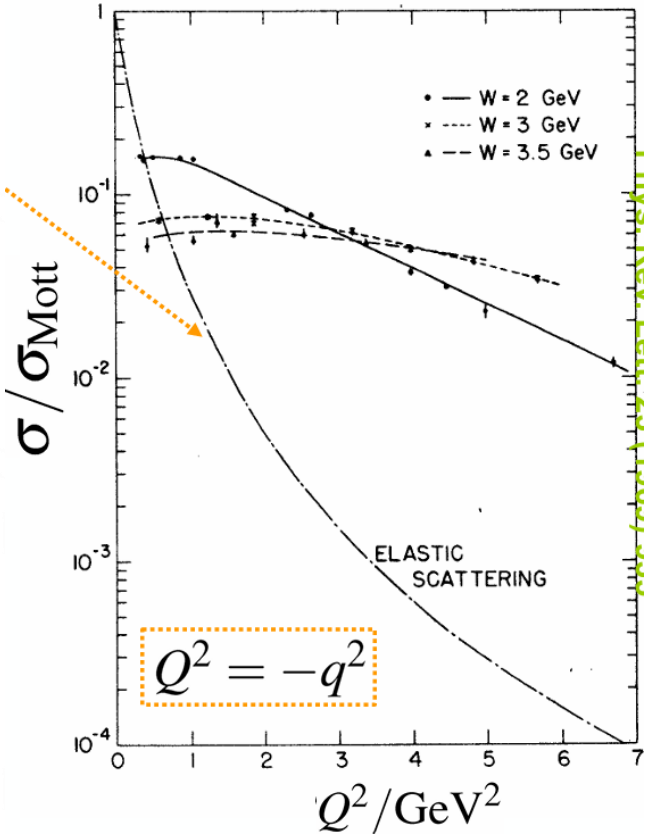

Structure functions

- Two independent functions are still needed to describes *DIS* cross section:
  - $\frac{d\sigma_{DIS}}{d\Omega dE'} = \left(\frac{d\sigma_M}{d\Omega}\right)\left(W_2(Q^2,\nu) + 2W_1(Q^2,\nu)\tan^2\theta/2\right)$,
- Note that $[W_{1,2}] = GeV^{-1}$. They are replaced by two dimensionless structure functions:
  - $F_1(x,Q^2) = MW_1(Q^2,\nu)$
  - $F_2(x,Q^2) = \nu W_2(Q^2,\nu)$

Note the change of variable $\nu \to x$

- $\frac{d\sigma_{DIS}}{d\Omega dE'} = \left(\frac{d\sigma_M}{d\Omega}\right)\frac{1}{\nu}\left(F_2(x,Q^2) + 2\frac{\nu}{M}F_1(x,Q^2)\tan^2\theta/2\right)$,

A bit of algebra...

$$\frac{d\sigma_{DIS}}{d\Omega dE'} = \left(\frac{d\sigma_M}{d\Omega}\right)\frac{1}{\nu}\left(F_2(x,Q^2) + 2\frac{\nu}{M}F_1(x,Q^2)\tan^2\theta/2\right)$$

$$= \left(\frac{d\sigma_M}{d\Omega}\right)\frac{1}{\nu}\left(F_2(x,Q^2) + 2\frac{\nu}{M}\frac{4MQ^2}{4MQ^2}F_1(x,Q^2)\tan^2\theta/2\right)$$

$$= \left(\frac{d\sigma_M}{d\Omega}\right)\frac{1}{\nu}\left(F_2(x,Q^2) + 2\frac{Q^2}{4M^2}\frac{4\nu\mathrm{M}}{Q^2}F_1(x,Q^2)\tan^2\theta/2\right)$$

$$= \left(\frac{d\sigma_M}{d\Omega}\right)\frac{1}{\nu}\left(F_2(x,Q^2) + 2\frac{Q^2}{4x^2M^2}x^2\frac{4\nu\mathrm{M}}{Q^2}F_1(x,Q^2)\tan^2\theta/2\right)$$

$$= \left(\frac{d\sigma_M}{d\Omega}\right)\frac{1}{\nu}\left(F_2(x,Q^2) + 2\frac{Q^2}{4x^2M^2}2xF_1(x,Q^2)\tan^2\theta/2\right)$$

Just one structure function of just one variable

- Two remarkable experimental evidences happen

1. $F_{1,2}$ do not depend on Q^2 *(Bjorkeen scaling)*
2. $2xF_1(x) = F_2(x)$ *(Callan Gross relation)*

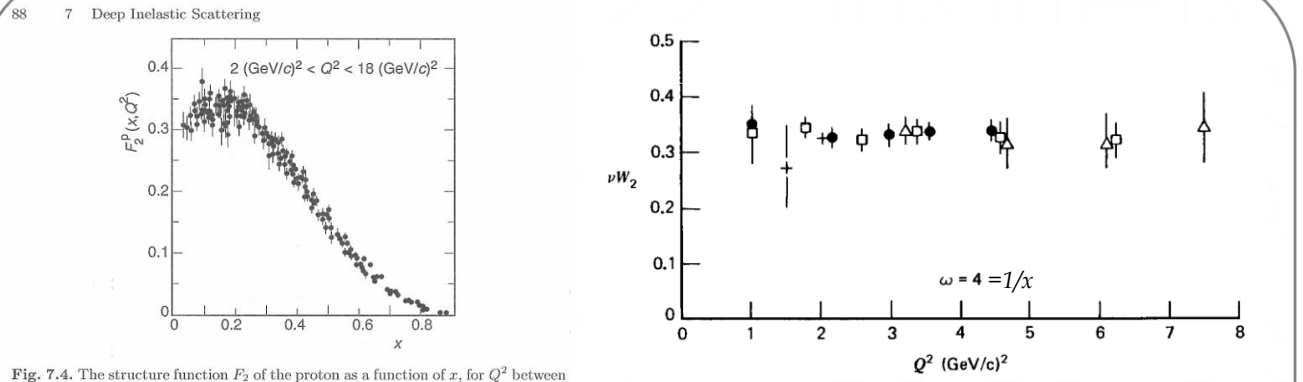

Fig. 7.4. The structure function F_2 of the proton as a function of x, for Q^2 between 2 (GeV/c)^2 and 18 (GeV/c)^2 [At82].

Two ways of representing **Bjorkeen scaling**:
- Left: the shape of $F_2(x)$ from data taken at different Q^2 is always the same
- Right: $F_2(x = \frac{1}{\omega} = 0.25)$ does not depend on Q^2

Callan-Gross relation

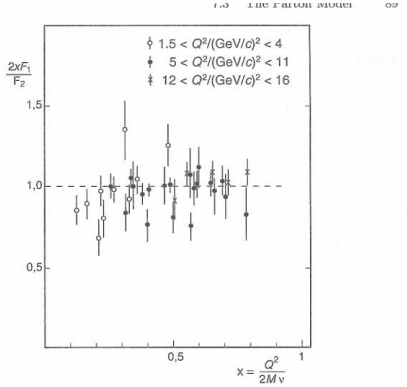

Fig. 7.5. Ratio of the structure functions $2xF_1(x)$ and $F_2(x)$. The data are from experiments at SLAC (from [Pe87]). It can be seen that the ratio is approximately constant (≈ 1).

Point-like "partons"

- Using the Callan Gross relation we can write:
  - $\frac{d\sigma_{DIS}}{d\sigma_M} \propto F_2(x)(1 + 2\frac{Q^2}{4m^2} \quad \tan^2\theta/2\,)$, with ***m=xM***

- Comparing to last eqn. on page 5 we may be tempted to reinterpret *DIS* as an *elastic interaction* of the electron with a *point-like, spin ½ ,* constituent of the proton *(a "parton"),* which carries a fraction *x=m/M* of its mass

- This interpretation holds true only in the "Breit" reference frame

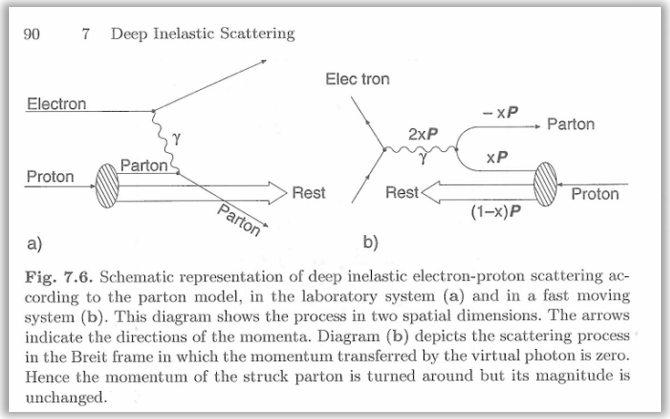

Fig. 7.6. Schematic representation of deep inelastic electron-proton scattering according to the parton model, in the laboratory system (a) and in a fast moving system (b). This diagram shows the process in two spatial dimensions. The arrows indicate the directions of the momenta. Diagram (b) depicts the scattering process in the Breit frame in which the momentum transferred by the virtual photon is zero. Hence the momentum of the struck parton is turned around but its magnitude is unchanged.

	Proton ↓	**Parton** ↓
Energy	E	xE
Momentum	p_L	xp_L
	$p_T = 0$	$p_T = 0$
Mass	M	$m = (x^2E^2 - x^2p_L^2)^{1/2} = xM.$

The parton picture

- Each nucleon is composed by point-like partons
- The probability of finding a parton of kind "i" with a fraction x of the nucleon momentum is described by a density function $f_i(x) =$
  - $u_v(x), d_v(x)$ for "valence" quarks, contributing to its quantum numbers
  - $g(x)$ for the gluons exchanged by quarks
  - $S(x)$ for "sea" q and $\bar{q}$ produced by gluon pair production
    - This includes also $s\bar{s}, c\bar{c}$, and even $b\bar{b}$ pairs.
    - We assume that the pdf for light sea quarks and antiquarks (u, d, s) be the same, $S(x)$
    - We neglect that of heavy c, b quarks, due their very large mass.
  - $S(x) = u_s(x) = \bar{u}_s(x) = d_s(x) = \bar{d}_S(x) = s(x) = \bar{s}(x)$

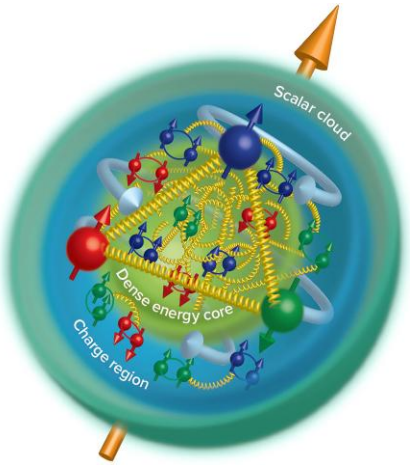

- Normalization condition: $\Sigma_i \, x f_i(x) = 1$
- $F_2(x)$ is the sum of the parton momentum distributions , weighted by their charges and momentum fraction:
  - $F_2(x) = x \cdot \Sigma_i \, z_i^2 f_i(x)$

$z^2 = 4/9\,, 1/9\,, 1/9, and\ 0\ for\ u(\bar{u}), d(\bar{d}), s(\bar{s}), and\ gluons$ respectively

A summary in pictures

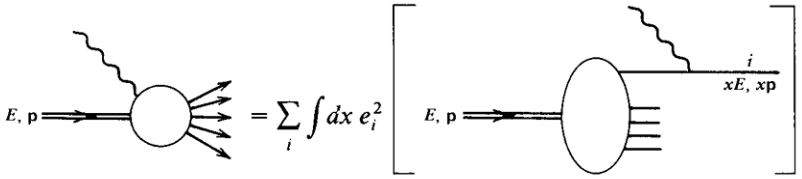

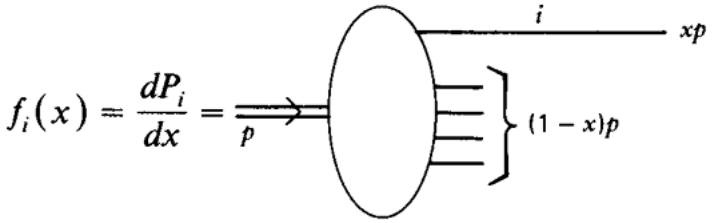

- The sum of the single particle energies, integrated over x must provide the proton momentum. This leads to the normalization condition:
  - $\Sigma_j \int dx\, p(x) f_j(x) = \Sigma_j \int dx\, (xP_N) f_j(x) = P_N$
  - $\Sigma_j \int dx\, x f_j(x) = 1$
- The sum extends over charged and neutral particles
  - The gluon *pdf* can be extracted by difference from unity

Useful relations

- $u_s(x) = \bar{u}_s(x) = d_s(x) = \bar{d}_s(x) = s_s(x) = \bar{s}_s(x) = S(x)$
- $u(x) = u_v(x) + u_s(x);\ d(x) = d_v(x) + d_s(x);\ s_v(x) = 0$

- Proton (*uud*) Sum Rules
  - $\int_0^1 [u^p(x) - \bar{u}^p(x)] = 2$
  - $\int_0^1 [d^p(x) - \bar{d}^p(x)] = 1$
- Neutron (*ddu*) Sum Rules
  - $\int_0^1 [u^n(x) - \bar{u}^n(x)] = 1$
  - $\int_0^1 [d^n(x) - \bar{d}^n(x)] = 2$

- Isospin symmetry exchange ($\boldsymbol{p \leftrightarrow n \equiv u \leftrightarrow d}$)
  - $u^p(x) = d^n(x) = u(p)$
  - $d^p(x) = u^n(x) = d(p)$

Nucleon Structure Function

- Proton *(uud)*, neutron *(udd)* :
  - $\frac{1}{x}F_2^p(x) = \left[\frac{4}{9}\,u_v^p(x) + \frac{1}{9}d_v^p(x) + \frac{4}{3}S(X)\right] = \frac{1}{9}[4u_v(x) + d_v(x)] + \frac{4}{3}S(x)$
  - $\frac{1}{x}F_2^n(x) = \left[\frac{1}{9}\,d_v^n(x) + \frac{4}{9}u_v^n(x) + \frac{4}{3}S(X)\right] = \frac{1}{9}[u_v(x) + 4d_v(x)] + \frac{4}{3}S(x)$

- Sea quarks are produced in pair by gluons, so they should mostly populate the low x region.
- We then expect for $\boldsymbol{R(x) = F_2^n(x)/F_2^p(x)}$:
  - $R(x) \to 1\ for\ x \to 1$ (mostly sea)
  - $R(x) \to \frac{u_v+4d_v}{4u_v+d_v} \simeq \frac{2}{3}\ for\ x \to 1$ (mostly valence)

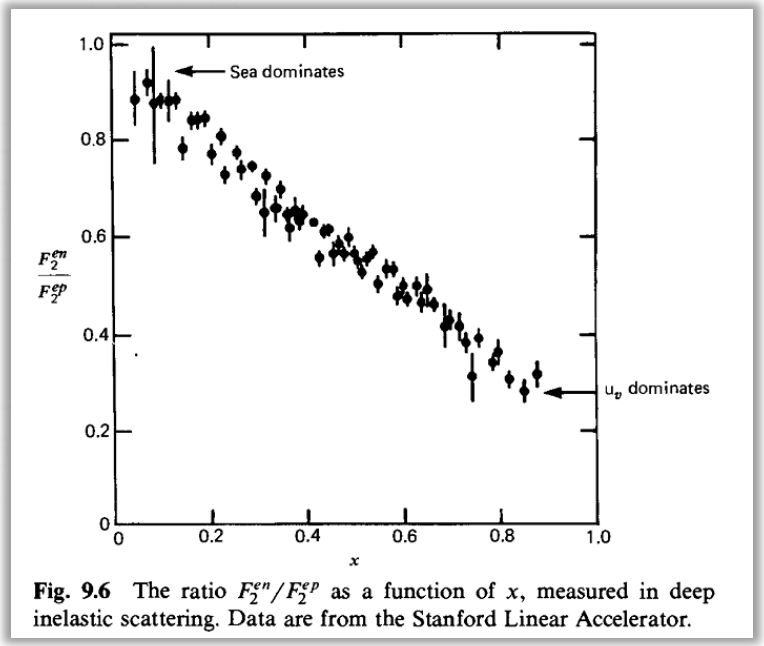

Fig. 9.6 The ratio F_2^{en}/F_2^{ep} as a function of x, measured in deep inelastic scattering. Data are from the Stanford Linear Accelerator.

Nucleon Structure Function

- Proton *(uud)*, neutron *(udd)* :
  - $\frac{1}{x}F_2^p(x) = \left[\frac{4}{9}\,u_v^p(x) + \frac{1}{9}d_v^p(x) + \frac{4}{3}S(X)\right] = \frac{1}{9}[4u_v(x) + d_v(x)] + \frac{4}{3}S(x)$
  - $\frac{1}{x}F_2^n(x) = \left[\frac{1}{9}\,d_v^n(x) + \frac{4}{9}u_v^n(x) + \frac{4}{3}S(X)\right] = \frac{1}{9}[u_v(x) + 4d_v(x)] + \frac{4}{3}S(x)$

- By subtracting the two function we get rid of the sea quark contribution:
  - $F_2^p(x) - F_2^n(x) = \frac{1}{3}[u_v(x) - d_v(x)]$

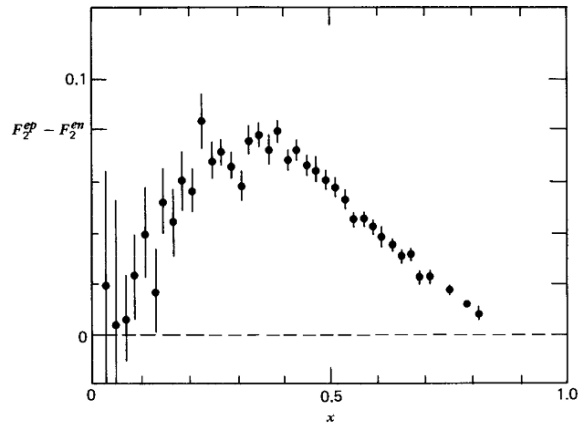

Fig. 9.8 The difference $F_2^{ep} - F_2^{en}$ as a function of x, as measured in deep inelastic scattering. Data are from the Stanford Linear Accelerator.

$\nu_\mu N \to \mu X$ DIS

- Further information is obtained from *charged current* interactions of *muon neutrino* and *antineutrino* beams
- Charge current allows only for:
  - $\nu_\mu d \to \mu^- u;\ \ \nu_\mu \bar{u} \to \mu^- \bar{d};\ \ \nu_\mu s \to \mu^- c$
  - $\bar{\nu}_\mu u \to \mu^+ d;\ \ \bar{\nu}_\mu \bar{d} \to \mu^+ \bar{u};\ \ \bar{\nu}_\mu \bar{s} \to \mu^+ \bar{c}$

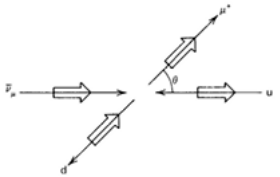

Fig. 12.13 The helicity configuration for high-energy $\bar{\nu}_\mu u \to \mu^+ d$ scattering.

- The chiral structure of *cc* weak interaction allows further disentangling *sea* and *valence* contribution to the structure function
  - Particles (ν, valence and sea q) interact with ***left*** chirality, i.e. ***negative*** helicity
  - Antiparticles ($\bar{\nu}$, sea $\bar{q}$) interact with ***right*** chirality, i.e. ***positive*** helicity
  - This affects ***total rates*** and ***spatial distributions***

Neutrino DIS in the CM frame

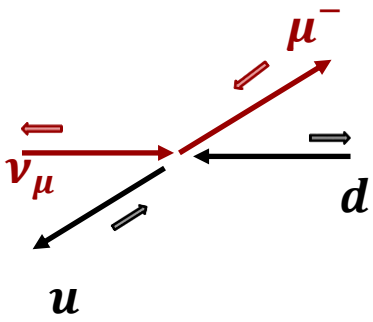

$\nu_\mu d \rightarrow \mu^- u$ interaction.
Left-neutrino hits left d-quark
$j_z = 0$: all directions are allowed

$$\frac{d\sigma}{ds\, d\cos\theta} = G_F^2 \frac{xs}{4\pi^2}$$

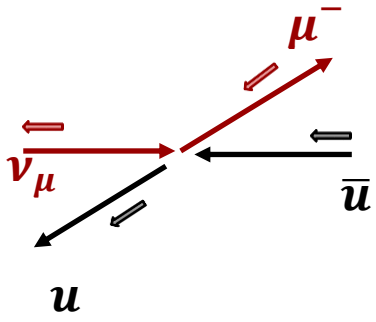

$\nu_\mu \bar{u} \rightarrow \mu^- d$ interaction.
Left-neutrino hits right $\bar{u}$-quark
$j_z = -1$: forward direction is favored

$$\frac{d\sigma}{ds\, d\cos\theta} = G_F^2 \frac{xs}{16\pi^2} (1 + \cos\theta)^2$$

For antineutrinos the opposite situation holds

$$\frac{d\sigma}{ds d\cos\theta} = \frac{G_F^2\, xs}{4\pi^2} \times f(\theta)$$

$f(\theta)$	Neutrino	Antineutrino
Quark	1	$(1+\cos\theta)^2/4$
Antiquark	$(1+\cos\theta)^2/4$	1

νscattering on isoscalar target

- Isoscalar nuclei: $N(p) = N(n) \rightarrow N(u) = N(d)$
- Neutrinos only interact with d *or* $\bar{u}$ quarks, so they measure:
  - $d^p(x) + d^n(x) = d(x) + u(x) = Q(x)$
  - $\bar{u}^p(x) + \bar{u}^n(x) = \bar{u}(x) + \bar{d}(x) = \bar{Q}(x)$
- We then have
  - $\frac{d\sigma}{dx\, d\cos\theta}\left(\nu_\mu N \rightarrow \mu^- X\right) = \frac{G_F^2 xs}{2\pi}\left[Q(x) + \frac{(1+\cos\theta)^2}{4}\bar{Q}(x)\right]$
  - $\frac{d\sigma}{dx\, d\cos\theta}\left(\bar{\nu}_\mu N \rightarrow \mu^+ X\right) = \frac{G_F^2 xs}{2\pi}\left[\bar{Q}(x) + \frac{(1+\cos\theta)^2}{4}Q(x)\right]$
- This allows disentangling the quark and antiquark components in the proton

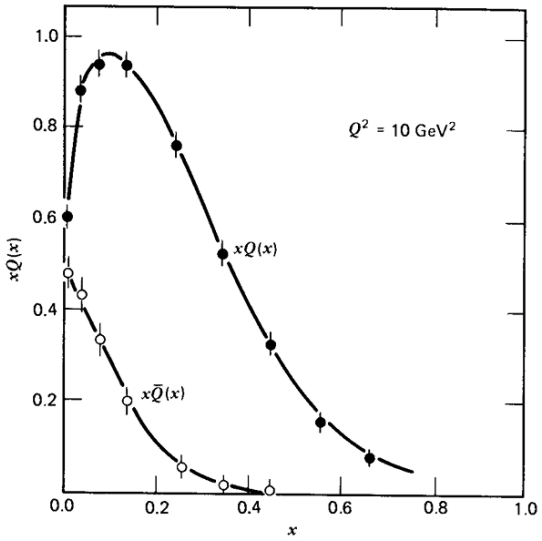

Fig. 12.14 Quark and antiquark momentum distributions in a nucleon as measured at CERN and the Fermi laboratory. The experiments reveal that only about half the proton's momentum is carried by quarks. We have associated the remainder with the gluon constituents (see Section 9.4).

nuTeV experiment at FNAL

- Proton beam hits a *BeO* target. In FNAL:
  - 800 GeV beam, 10^{13}p/spill, 1 spill minute
  - Overall accumulated ~10^{18} Protons On Target (pot)
- $p\ BeO\ \rightarrow \pi^{\pm}, K^{\pm}, etc$
  - Bending magnets select the charge of the hadron(either + or -)
  - $\pi^{\pm}$ fly in a decay tunnel and then decay $\pi^{+} \rightarrow \mu^{+}\nu_{\mu}$ (or cc)
  - An absorbed filters away the muons, leaving just a neutrino or antineutrino beam

nuTeV experiment at FNAL

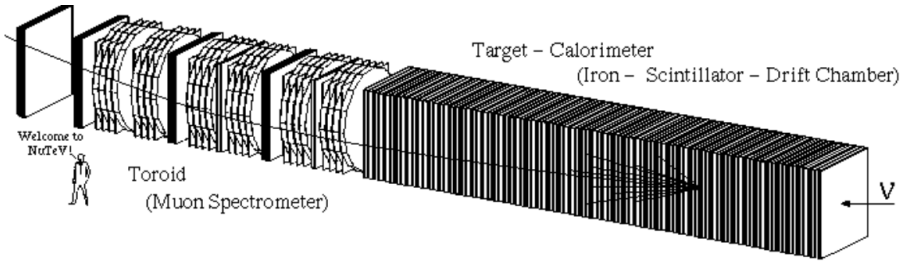

- The detector consist in a calorimeter, a dense iron absorber where neutrinos interact, instrumented with scintillator material which absorbs and reconstructs the hadron shower
- A toroidal magnetic field equipped with drifts chambers tracks the charged muon, measures its trajectory and momentum

ν_μ

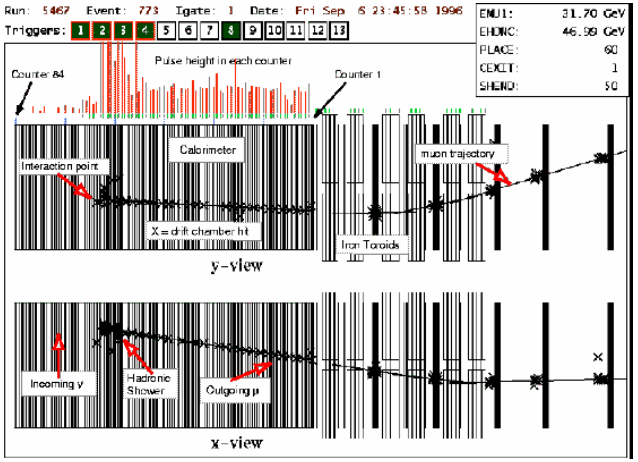

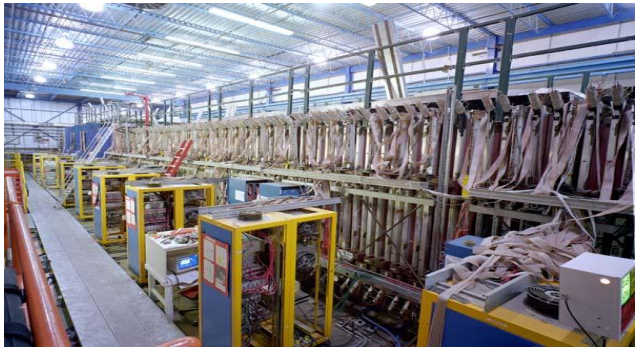

Summary

- By combining the results from several experiments of charge and neutral leptons scattering on nucleons a precise description of the *pdf*s of *valence quarks, sea quarks and antiquarks, and gluons* inside the nucleon is obtained
- These are used as input to parameterize *pp* scattering at the LHC and compute cross sections

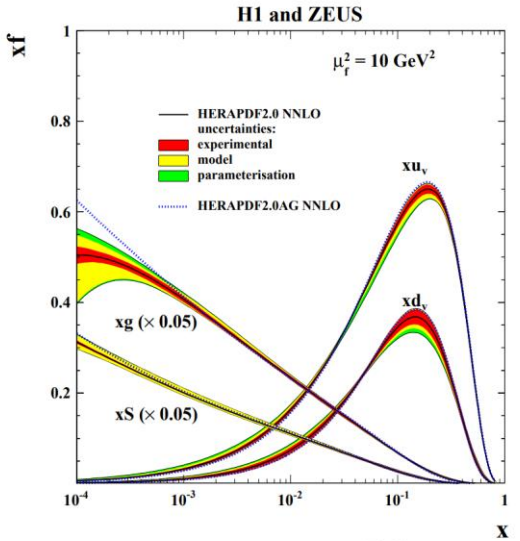

Figure 23: The parton distribution functions xu_v, xd_v, $xS = 2x(\bar{U}+\bar{D})$ and xg of HERAPDF2.0 NNLO at $\mu_f^2 = 10\,\mathrm{GeV}^2$. The gluon and sea distributions are scaled down by a factor 20. The experimental, model and parameterisation uncertainties are shown. The dotted lines represent HERAPDF2.0AG NNLO with the alternative gluon parameterisation, see Section 6.8.

Scaling violations

- The independence of $F_2(x)$ *on* Q^2 ("Bjorkeen scaling") is only true in a limited range of momenta
- QCD predicts violations from this law, parameterized by "DGLAP" equations
- Measurements performed at HERA confirm this picture providing a strong confirmation of QCD predictions

